Prediction of the Non-Isothermal Shrinkage of Natural Clay through a Fully Coupled Thermo-Hydro-Mechanical Model

Omid Ghasemi-Fare, Ph.D., A.M.ASCE¹; and Mohammadreza Mir Tamizdoust, A.M.ASCE²

¹Associate Professor, Dept. of Civil and Environmental Engineering, Univ. of Louisville, Louisville. Email: omid.ghasemifare@louisville.edu

²Geotechnical Engineer, Dept. of Forensic Engineering, Bryant Consultants Operating, Carrollton, TX. Email: ktamizdoust@geoneering.com

ABSTRACT

Underground geo-structures and climate change can trigger heat, moisture, and vapor flow and may induce volumetric shrinkage in clays. This drying phenomenon is a multiphysical process and is accompanied by alterations in the thermal, hydraulic, and mechanical states of the multiphase system. Reversible and irreversible characteristics of shrinkage deformation have been observed experimentally in clayey for different ranges of moisture contents. An accurate evaluation of the drying process helps to study the drying-induced damage of geomaterials. In this study, a finite element model that considers the thermo-poroelastoplastic constitutive framework is developed. The developed thermo-hydro-mechanical (THM) model can accurately analyze the transversely isotropic behavior of natural clays in unsaturated conditions. Results indicate that 82% of the total volumetric deformation in dying-induced shrinkage is irrecoverable. In addition, it is observed that most of the plastic volume change occurs within the early stage of drying when the soil's unsaturated condition is in a funicular state.

KEYWORDS: THM modeling, Clays, thermal shrinkage; Constitutive modeling

INTRODUCTION

When saturated or partially saturated fine-grained soils are subjected to a high suction, they begin to desaturate which consequently leads to the shrinkage of the material (Tamizdoust and Ghasemi-Fare, 2022a, b, c). In other words, the gradient between the relative humidity (and/or temperature) of the environment and soil drives the drying (dehydration) process, where liquid within the soil evaporates and migrates to the evaporative boundary (Bittelli et al., 2008; Gerard et al., 2010; Tamizdoust et al., 2020). This process may induce a non-uniform moisture variation in the soil which can lead to drying-induced shrinkage and, consequently, desiccation cracks (Peron et al., 2013). The presence of cracks in soils will also create weak zones which result in a reduction in mechanical strength and bearing capacity and increases compressibility. Thus, mechanical engineering properties and stability of buildings and structures that are constructed on clayey soils would be affected by thermal shrinkage. The shrinkage drying is an important concern for geotechnical infrastructures (Bordoloi et al., 2018; Feng et al., 2017; Lai et al., 2019) including embankments (Lai et al., 2019; McMahon et al., 2020), and landfill covers (Li et al., 2016; Shaikh et al., 2019). Given the importance of this problem in geotechnical engineering, the drying-induced shrinkage has been the subject of many theoretical and experimental studies (Ghorbani et al., 2009; Hedan et al., 2012; Ng and Leung, 2012; Sánchez et al., 2014; Vesga, 2008). It has been observed experimentally that, large irrecoverable (plastic) deformations occur at the beginning of the desaturation process (where the degree of saturation is above 95% and around air-entry suction value). Conventional geotechnical laboratory tests on natural and compacted fine-grained soils denote that in the case of drying, clayey soils undergo volume reduction; on the other hand, during wetting, they experience expansion (swelling) (Alonso et al., 2005; Cherati and Ghasemi-Fare, 2021; Coccia and McCartney, 2016; Joshaghani and Ghasemi-Fare, 2021; Romero et al., 2011; Tamizdoust and Ghasemi-Fare, 2020; Viola et al., 2005).

In this study, a fully-coupled thermo-hydro-mechanical (THM) model is developed to analyze the non-isothermal shrinkage of a natural clay considering a transversely isotropic thermo-elastoplastic constitutive model. This paper evaluates the accuracy of a THM model developed in COMMSOL utilized to model the fast drying of clays. The model can be used to study the drying of clayey soils.

Mathematical Model Description

In this research, the finite element model considers the unsaturated anisotropic thermo-poroelastoplastic constitutive model based on Bishop's stress (average skeleton stress) variable and the fourth-order projection tensor approach. The developed model strongly couples the mass balances of liquid water, and water vapor, the balance of thermal energy, and stress equilibrium that are presented in Equations (1) to (3) (Coussy, 2004; Tamizdoust and Ghasemi-Fare, 2022b).

$$n\rho_{l}\left[S_{l}c_{l}+C_{p}\right]\frac{\partial p_{l}}{\partial t}+\nabla\cdot\left(nS_{l}\rho_{l}v_{l}-D_{v}\nabla\rho_{v,eq}\right)=\rho_{l}S_{l}\left[n\alpha_{l}\frac{\partial T}{\partial t}-\left(1-n\right)\frac{\partial\varepsilon_{v}}{\partial t}\right]$$
(1)

$$(\rho C)_{m} \frac{\partial T}{\partial t} - \lambda_{m} \nabla^{2} T = -L_{v} \left\{ \frac{\partial \left[n \left(1 - S_{l} \right) \rho_{v,eq} \right]}{\partial t} + \nabla \cdot \left(-D_{v} \nabla \rho_{v,eq} \right) \right\}$$
(2)

$$\nabla . \mathbf{\sigma} + \rho_{\mathbf{b}} \mathbf{g} = \mathbf{0} ; \mathbf{\sigma} = \mathbf{\sigma}' + p_{g} \mathbf{I} - \chi \left(S_{l} \right) p_{c} \mathbf{I} ; \qquad \chi \left(S_{l} \right) = S_{l}$$
(3)

In Equations (1) to (3) n (m³/m³) is the porosity of the medium, and S_l is the degree of saturation of water. C_p (1/Pa) is the moisture capacity and can be derived from the Soil Water Characteristic Curve (SWCC) curve. ρ_l , (kg/m³) is the density of water, and $\rho_{v,eq}$ is the equilibrium vapor density. Moreover, D_v (m².s⁻¹) is the effective diffusivity. c_l is (MPa) is the compressibility modulus of water, and α_l (1/°C) is the linear thermal expansion of water. σ and Γ are stress and identity tensors, and Γ is Bishop's effective stress factor. \vec{m} (kg/m³/s) is denoted as the rate of phase change. T(K) is the temperature of the medium, (ρC)_m (J/K/m³) is the volumetric heat capacity, and λ_m (W/K/m²) is the thermal conductivity of the medium which both depend on the porosity, degree of saturation, and thermal conductivity (specific heat capacity) of the liquid water, vapor, and solid soil. Moreover, L_v (J/kg) is the latent heat of vaporization.

In this study, the unsaturated fluid flow in a transversely isotropic medium is governed by the Darcy's flow:

$$nS_l v_l = -\frac{\mathbf{\kappa}_{int} \kappa_{rl}}{\mu_l} (\nabla p_l + \rho_l g)$$
(4)

Where μ l (Pa.s) is the dynamic viscosity of water, κ_{rl} (-) is the relative permeability of water, and κ_{int} (m2) is the second-order intrinsic permeability tensor of the medium defined as:

$$\mathbf{\kappa}_{\text{int}} = \kappa_{\text{int},\perp} \mathbf{m} + \kappa_{\text{int},\parallel} (1 - \mathbf{m}) \tag{5}$$

Where $\kappa int, \parallel$ and $\kappa int, \perp$ (m2) are the intrinsic permeability components, respectively, parallel and perpendicular to the bedding planes.

Moreover, the VG model is incorporated into the developed model. It is to be noted that phase change in fine grain soils happens almost instantaneously; therefore, an equilibrium phase change approach is adopted. In the equilibrium phase change approach, the mass balance of liquid and vapor diffusion are combined (Equation 1), and the gas mass balance is disregarded.

Numerical Model

To study the convective drying of clays, the provided coupled equations governing multiphase flow in deformable soils are simultaneously solved using the COMSOL Multiphysics software v5.3a (COMSOL, 2018). According to Prime et al. (Prime et al., 2015) in order to accurately model the evaporation process in Boom clay, an orthotropic model must be used. Therefore, a 3D cylindrical domain is considered. The experimental results on the non-isothermal shrinkage of Boom clay are used to validate the developed model. The model is discretized using hexahedral elements in COMSOL.

Figure 1 presents the finite element mesh. The radius and height of the numerical model (R=6.73 mm, and H= 6 mm) are selected based on the experiment. A saturated and stress-free clay sample with an initial temperature of 17 °C is considered. The initial and boundary conditions of the sample are presented in Figure 1. The bottom boundary is restrained in the z direction, while all other boundaries are free to move. According to the experimental model, only the top surface is exposed to the environment and thus evaporation (heat and mass flow) occurs only from the top surface. The extremely low relative humidity of the environment drives the evaporation and drying process from the top surface of the sample. The air temperature is 25°C and the relative humidity of the air is 3.5%. The low relative humidity induces a high suction value at the top surface.

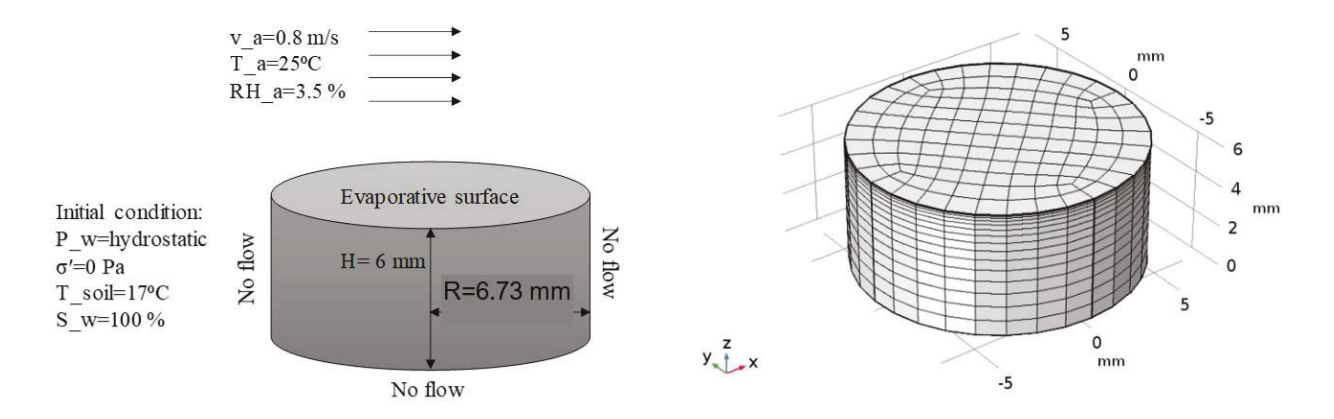


Figure 1. Finite Element Domain and boundary conditions

Table 1 present the properties of the clay used in the presented model. All the parameters are borrowed from the literature. Parameters related to yielding and stress-dilatancy are obtained from triaxial test results performed by Sultan et al. (2010) on natural Boom clay.

Parameter	Values	Units	Parameter	Values	Units
n_0	0.39	m^3/m^3	C_{w}	4185	J/kg/°C
$\kappa_{0int, }$	5×10 ⁻¹⁹	m^2	C_{g}	2062	J/kg/°C
$\kappa_{oint,\perp}$	2.5×10 ⁻¹⁹	m^2	$C_{\rm s}$	750	J/kg/°C
μ_{w}	0.001	Pa.s	λ_{l}	0.59	W/m/°C
c_1	4.5×10 ⁻¹⁰	1/Pa	$\lambda_{ m g}$	0.026	W/m/°C
ρ_{s}	2670	kg/m ³	$\lambda_{\rm s}$	1.7	W/m/°C
ρ_{w0}	998.2	kg/m ³	α_1	3×10 ⁻⁴	1/°C

Table 1. Thermohydraulic properties of the selected clay

RESULTS

An initially saturated Boom clay is considered which undergoes convective drying while no external total stress is applied. The drying rate and mass loss in the clay sample are compared with experimental results obtained by Prime et al. (Prime et al., 2015). The comparison shows that the preliminary model can accurately predict the evaporation and drying process in clays. Figure 2 compares the drying kinetics in terms of the weight loss, and drying rate as a function of the gravimetric water content. The drying rate is calculated using the rate of mass loss (dm/dt [kg/s]) divided by the top surface $(S(t) [m^2])$ which is updated at each step due to the thermal volume shrinkage.

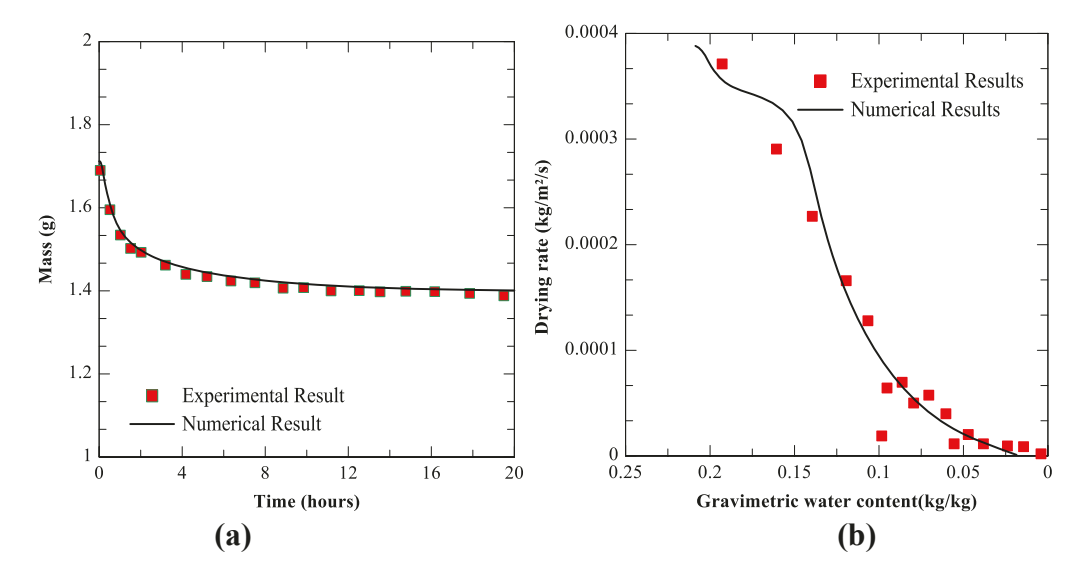


Figure 2. Comparison of numerical and experimental models, a) Mass loss, and c) Drying rate as a function of water content

The drying rate and the drying-induced volume shrinkage are also predicted using the developed model. Figure 3(a) presents the comparison of the drying rate obtained from the

numerical model with the experimental observations. This comparison confirms the capability of the developed model to analyze the total volume shrinkage during the drying process. The total volume shrinkage obtained from the numerical model is presented in Figure 3(b). As it can be seen in Figure 3 there is an abrupt decrease in the drying rate and thus a sudden decrease in total volume at the beginning of the drying process. The comparison of the elastic and plastic deformations obtained from the numerical model indicates that the drying shrinkage results in a 30% volume reduction drying-induced shrinkage in which approximately 82% of the total volume deformation is irrecoverable (i.e., plastic).

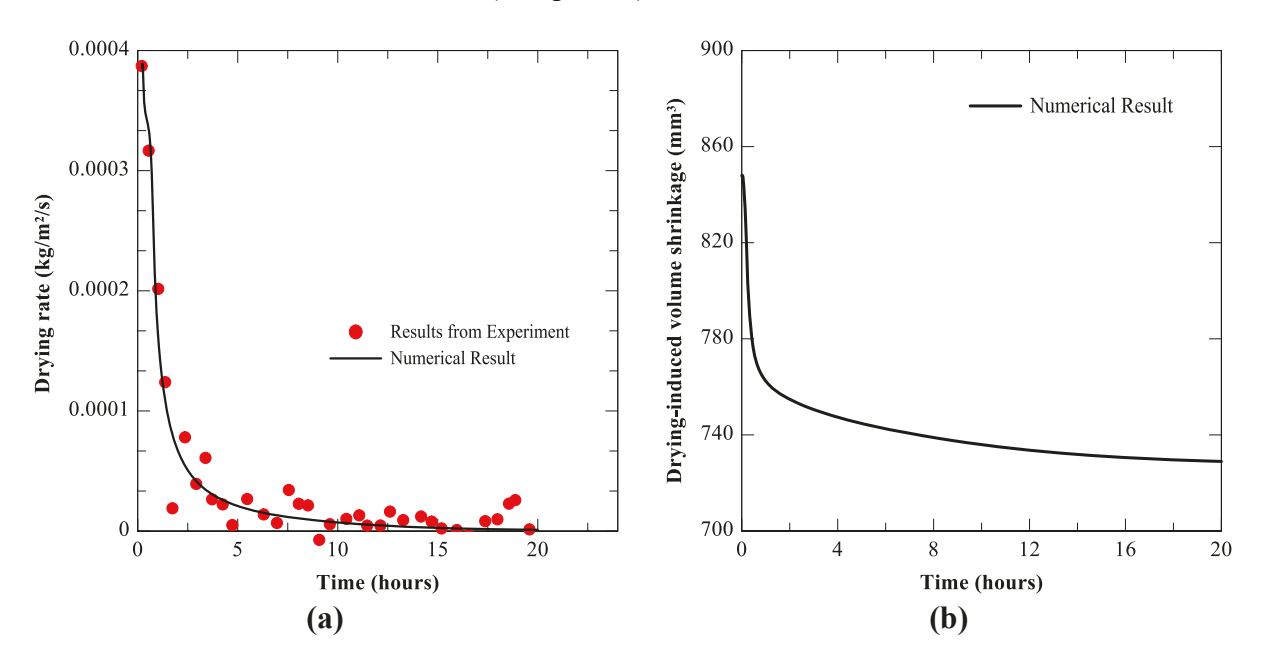


Figure 3. Prediction of (a) drying rate, and b) Total volume shrinkage during the drying test

In the following the variations of the degree of saturation, and schematic volume shrinkage are studied. Figure 4 shows the changes in the degree of saturation during the drying process. As it can be seen, shortly after the convective drying (after 1 hour), the degree of saturation or water content distribution within the sample is non-uniform. The results show over 60% difference between the degrees of saturation at the top which is 20.1% and at the bottom of the sample which is 81.4%. However, after 20 hours of convective drying, most of the water evaporates from the sample and the soil skeleton reaches an equilibrium condition. At this time, almost uniform water content is observed in which the variation in the degree of saturation is less than 1.5%.

The validated model is used to analyze the volume shrinkage and evaporation volume (water loss) during the drying process. The evaporation volume is calculated as mass loss divided by the water density and the shrinkage volume is the difference between the total volume at each step (which was shown in Figure 3b) and the initial volume. Figure 5 demonstrates that the shrinkage volume and water loss follow the same trend (linear reduction) until the gravimetric water content equals 0.2. This indicates that during the early stage of drying the volume of the evaporated water is identical to the sample contraction (i.e., porosity reduction is equal to water loss). This phenomenon is called Normal shrinkage which implies evaporation occurs without desaturation. However, beyond this point due to the drying-induced shrinkage, the slope of the

soil shrinkage is reduced while the slope of evaporation volume against the gravimetric water content is still linear. The comparison of the experimental and numerical results confirms the capability of the developed model in predicting the drying process in deformable porous media.

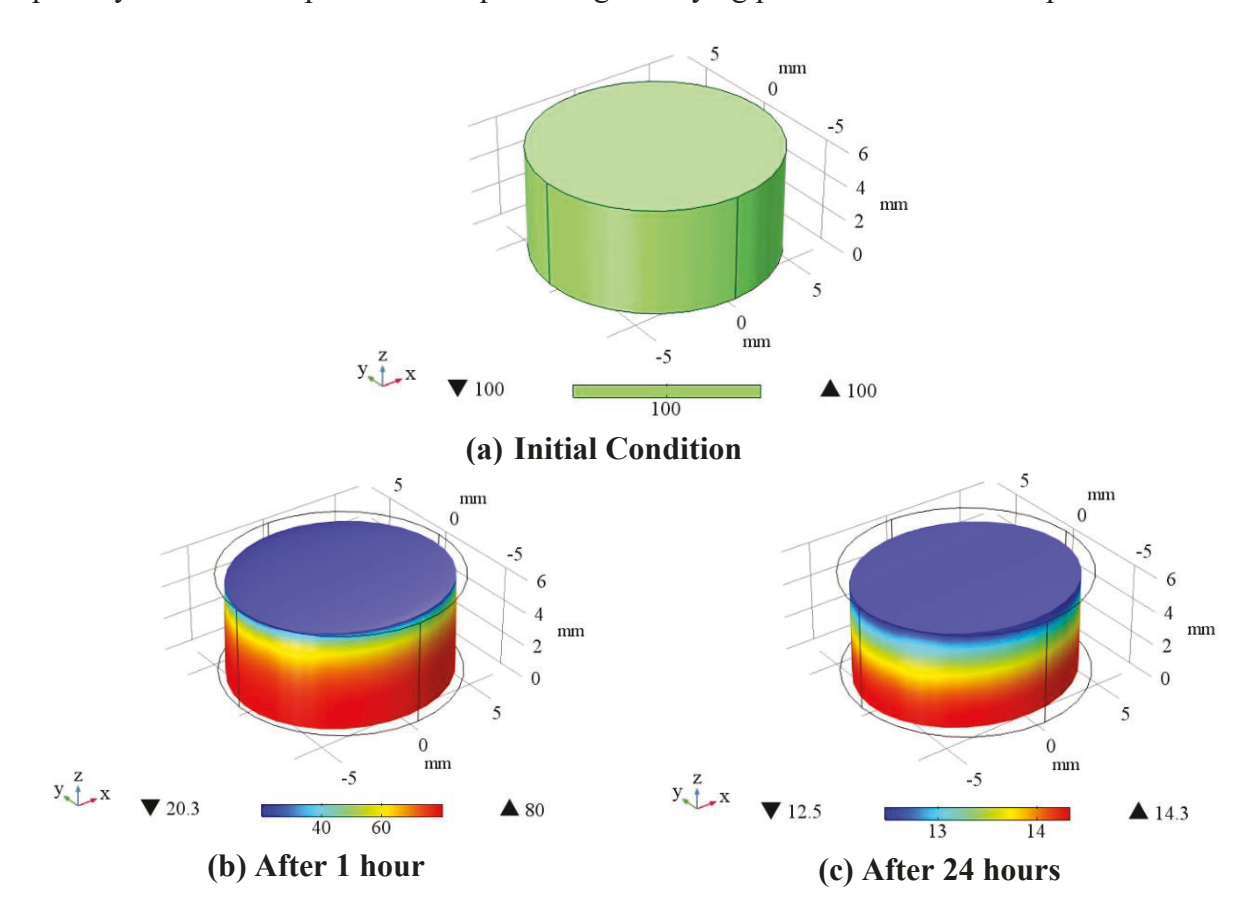


Figure 4. Drying-induced volume shrinkage and reduction in moisture content, (a) initial condition, b) after 1 hour of convective drying, and c) after 24 hours of convective drying

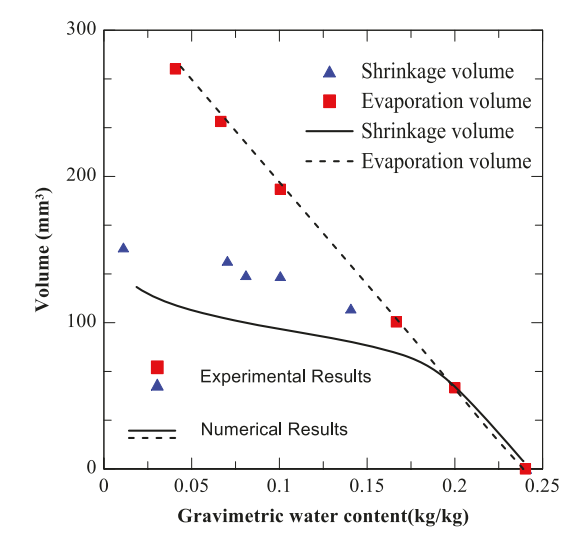


Figure 5. Comparison of the volumetric evaporation and shrinkage curves

CONCLUSIONS

In this paper, a finite element model is developed to analyze the drying-induced shrinkage of a transversely isotropic clay. The comparison of the numerical and experimental results indicates that the developed THM model can accurately predict the drying process in deformable porous media. Numerical results show a non-uniform degree of saturation (a 60% difference in the degree of saturation) within the sample during the early stage of drying, while uniform water content distribution is observed after 20 hours. Furthermore, it has been observed that most of the drying-induced volume reduction (nearly 80% of the volume shrinkage) is plastic deformation and occurs at the early stage of drying (within the first 2 hours of drying).

ACKNOWLEDGEMENT

The authors would also like to gratefully acknowledge the financial support by the National Science Foundation under Grant No. CMMI-1804822.

REFERENCES

- Alonso, E., Romero, E., Hoffmann, C., and García-Escudero, E. 2005. Expansive bentonite—sand mixtures in cyclic controlled-suction drying and wetting. *Engineering Geology* 81, 213-226.
- Bittelli, M., Ventura, F., Campbell, G. S., Snyder, R. L., Gallegati, F., and Pisa, P. R. 2008. Coupling of heat, water vapor, and liquid water fluxes to compute evaporation in bare soils. *Journal of Hydrology* 362, 191-205.
- Bordoloi, S., Hussain, R., Gadi, V., Bora, H., Sahoo, L., Karangat, R., Garg, A., and Sreedeep, S. 2018. Monitoring soil cracking and plant parameters for a mixed grass species. *Géotechnique Letters* 8, 49-55.
- Cherati, D. Y., and Ghasemi-Fare, O. 2021. Unsaturated thermal consolidation around a heat source. *Computers and Geotechnics* 134, 104091.
- Coccia, C. J. R., and McCartney, J. S. 2016. Thermal volume change of poorly draining soils I: Critical assessment of volume change mechanisms. *Computers and Geotechnics* 80, 26-40.
- COMSOL. 2018. *COMSOL Multiphysics v.5.3a*. COMSOL AB, Stockholm, Sweden: www.comsol.com.
- Coussy, O. 2004. Poromechanics. John Wiley & Sons.
- Feng, S., Leung, A. K., Ng, C. W. W., and Liu, H. 2017. Theoretical analysis of coupled effects of microbe and root architecture on methane oxidation in vegetated landfill covers. *Science of the Total Environment* 599, 1954-1964.
- Gerard, P., Léonard, A., Masekanya, J.-P., Charlier, R., and Collin, F. 2010. Study of the soil—atmosphere moisture exchanges through convective drying tests in non-isothermal conditions. *International Journal for Numerical and Analytical Methods in Geomechanics* 34, 1297-1320.
- Ghorbani, A., Zamora, M., and Cosenza, P. 2009. Effects of desiccation on the elastic wave velocities of clay-rocks. *International Journal of Rock Mechanics and Mining Sciences* 46, 1267-1272.
- Hedan, S., Cosenza, P., Valle, V., Dudoignon, P., Fauchille, A.-L., and Cabrera, J. 2012. Investigation of the damage induced by desiccation and heating of Tournemire argillite using digital image correlation. *International Journal of Rock Mechanics and Mining Sciences* 51, 64-75.

- Joshaghani, M., and Ghasemi-Fare, O. 2021. Exploring the effects of temperature on intrinsic permeability and void ratio alteration through temperature-controlled experiments. *Engineering Geology* 293, 106299.
- Lai, D., Liu, W., Gan, T., Liu, K., and Chen, Q. 2019. A review of mitigating strategies to improve the thermal environment and thermal comfort in urban outdoor spaces. *Science of The Total Environment* 661, 337-353.
- Li, J., Li, L., Chen, R., and Li, D. 2016. Cracking and vertical preferential flow through landfill clay liners. *Engineering Geology* 206, 33-41.
- McMahon, J. M., Olley, J. M., Brooks, A. P., Smart, J. C., Stewart-Koster, B., Venables, W. N., Curwen, G., Kemp, J., Stewart, M., and Saxton, N. 2020. Vegetation and longitudinal coarse sediment connectivity affect the ability of ecosystem restoration to reduce riverbank erosion and turbidity in drinking water. *Science of The Total Environment* 707, 135904.
- Ng, C. W. W., and Leung, A. K. 2012. Measurements of drying and wetting permeability functions using a new stress-controllable soil column. *Journal of Geotechnical and Geoenvironmental Engineering* 138, 58-68.
- Peron, H., Laloui, L., Hu, L.-B., and Hueckel, T. 2013. Formation of drying crack patterns in soils: a deterministic approach. *Acta Geotechnica* 8, 215-221.
- Prime, N., Levasseur, S., Miny, L., Charlier, R., Léonard, A., and Collin, F. J. C. G. J. 2015. Drying-induced shrinkage of Boom clay: an experimental investigation, *Canadian Geotechnical Journal*. 53, 396-409.
- Romero, E., Della Vecchia, G., and Jommi, C. 2011. An insight into the water retention properties of compacted clayey soils. *Géotechnique* 61, 313-328.
- Sánchez, M., Manzoli, O. L., and Guimarães, L. J. 2014. Modeling 3-D desiccation soil crack networks using a mesh fragmentation technique. *Computers and Geotechnics* 62, 27-39.
- Shaikh, J., Bordoloi, S., Yamsani, S. K., Sekharan, S., Rakesh, R. R., and Sarmah, A. K. 2019. Long-term hydraulic performance of landfill cover system in extreme humid region: Field monitoring and numerical approach. *Science of the total environment* 688, 409-423.
- Sultan, N., Cui, Y.-J., and Delage, P. 2010. Yielding and plastic behaviour of Boom clay. *Géotechnique* 60, 657-666.
- Tamizdoust, M. M., and Ghasemi-Fare, O. 2020. A fully coupled thermo-poro-mechanical finite element analysis to predict the thermal pressurization and thermally induced pore fluid flow in soil media. *Computers and Geotechnics* 117, 103250.
- Tamizdoust, M. M., and Ghasemi-Fare, O. 2022a. Assessment of thermal, hydraulic, and mechanical constitutive relations on the temperature-induced stress and pore fluid pressure in saturated clays. *Computers and Geotechnics* 145, 104686.
- Tamizdoust, M. M., and Ghasemi-Fare, O. 2022b. Convective Drying Analysis of Transversely Isotropic Natural Clay. *Journal of Geotechnical and Geoenvironmental Engineering* 148, 04022073.
- Tamizdoust, M. M., and Ghasemi-Fare, O. 2022c. Long-term Thermo-hydraulic Response of the Shallow Subsurface soil in the Vicinity of a Buried Horizontal Heat Source. *International Journal of Heat and Mass Transfer* 183, 122120.
- Tamizdoust, M. M., Moradi, A., and Ghasemi-Fare, O. 2020. Numerical Analysis of variation of saturation and moisture transport at the vicinity of a heat source, *Geo-Congress 2020: Geo-Systems, Sustainability, Geoenvironmental Engineering, and Unsaturated Soil Mechanics*. American Society of Civil Engineers Reston, VA, pp. 349-357.

- Vesga, L. 2008. Equivalent effective stress and compressibility of unsaturated kaolinite clay subjected to drying. *Journal of geotechnical and geoenvironmental engineering* 134, 366-378.
- Viola, R., Tuller, M., Or, D., and Drasdis, J. 2005. Microstructure of clay-sand mixtures at different hydration states. In *Proceedings of International Symposium on Advanced Experimental Unsaturated Soil Mechanics, Trento, Italy*, In: Tarantino A, Romero E, Cui YJ (eds) Advanced experimental unsaturated soil mechanics, Taylor, Francis Group, London, 437-442.